Biochemical Pharmacology 192 (2021) 114719

Contents lists available at ScienceDirect

Biochemical Pharmacology

journal homepage: www.elsevier.com/locate/biochempharm

Activation of Nrf2 by methylene blue is associated with the neuroprotection against MPP^+ induced toxicity via ameliorating oxidative stress and mitochondrial dysfunction

Sunil Bhurtel [a,1], Eugene Bok [b,1], Nikita Katila [a], Jaekwang Kim [b,*], Dong-Young Choi [a,*]

[a] College of Pharmacy, Yeungnam University, 280 Daehak-Ro, Gyeongsan, Gyeongbuk 38541, Republic of Korea
[b] Dementia Research Group, Korea Brain Research Institute, Daegu 41062, Republic of Korea

ARTICLE INFO

Keywords:
MPP^+
Parkinson's disease
Methylene blue
Oxidative stress
Mitochondria

ABSTRACT

The neuropathological hallmark of Parkinson's disease (PD) is the preferential loss of dopaminergic neurons in the substantia nigra and presence of Lewy bodies in the dying neurons. Though specific molecular mechanisms for the neurodegeneration remains to be clarified, mitochondrial dysfunction and increased oxidative stress are major players associated with PD pathogenesis and these pathogenic mechanisms can be reproduced in cells and animals by application of various neurotoxins such as MPP^+. In this study, we attempted to determine the neuroprotective effects of methylene blue (MB) against 1-methyl-4-phenylpyridinium (MPP^+)-induced neurotoxicity, and to elucidate its action mechanism. We observed that MB attenuated MPP^+-induced apoptotic cell death in SH-SY5Y cells and the mescencephalic dopaminergic neurons. In addition, MB protected the cells against MPP^+-induced oxidative stress and mitochondrial dysfunction as evidenced by restoration of mitochondrial complex I activity and ATP levels, and attenuation of oxidative stress. Moreover, we demonstrated that MB induced antioxidant molecules, and activated Nrf2 pathway through AKT activation. These results indicate that MB protects the neurons from MPP^+-induced toxicity through activation of antioxidant system, thereby reducing the oxidative stress and mitochondrial impairment, implying the potential use of MB in the treatment of neurodegenerative diseases such as PD.

1. Introduction

Parkinson's disease (PD) is the second most common neurodegenerative disorder with a global prevalence of about 6.1 million patient [1]. The pathological hallmark of PD is a selective and pronounced loss of the dopaminergic neurons in the ventral mesencephalic substantia nigra pars compacta resulting in drastic depletion of dopamine in the striatum [2,3]. However, the molecular mechanisms by which the dopaminergic neurons die remain elusive. Accumulating evidence from human studies and various experimental models for PD indicate that mitochondrial dysfunction and oxidative stress might play a pivotal role for the dopaminergic neuronal loss [4]. Mitochondrial dysfunction and oxidative stress in PD can be mimicked using the neurotoxin 1-methyl-4-phenyl-1,2,3,6-tetrahydropyridine (MPTP). MPP^+, a toxic metabolite of MPTP is taken up into the dopaminergic neurons via the dopamine transporter and inhibits mitochondrial complex I, resulting in overproduction of the superoxide radical [5], decrease in ATP production [6] and ultimate death of the dopaminergic neurons [7].

Since decreased mitochondrial complex I activity was found in PD patients [4,8], researchers have observed different types of mitochondrial impairments in PD patients, including decreased mitochondrial membrane potential [9], and imbalances in mitochondrial fission and fusion [10]. Futhermore, mutations and underexpression of genes encoding proteins that are relevant for mitochondrial homeostasis have been exhibited to be unequivocally linked to PD. One of them is peroxisome proliferator–activated receptor γ coactivator-1α (PGC-1α), a master regulator of mitochondrial biogenesis and oxidative metabolism [11,12]. Mitochondrial dysfunction not merely exerts ATP depletion, but also rise in generation of reactive oxygen species (ROS), causing detrimental cellular alterations, including protein carbonylation, lipid peroxidation, an increase in misfolding and aggregation of proteins such as α-syn, and cytochrome (cyt) c release into the cytosol which results in

* Corresponding authors.
E-mail addresses: kim_jaekwang@kbri.re.kr (J. Kim), dychoi@yu.ac.kr (D.-Y. Choi).
[1] S. Bhurtel and E. Bok contributed equally to this article.

https://doi.org/10.1016/j.bcp.2021.114719
Received 28 July 2021; Received in revised form 30 July 2021; Accepted 30 July 2021
Available online 2 August 2021

caspase activation and apoptotic cell death [10,13-15].

Mitochondria have their own system to detoxify the superoxide anions which are generated at complex I and complex III of the mitochondrial respiratory chain known as superoxide dismutase (SOD). The cytosolic SOD (Cu/Zn SOD) or mitochondrial SOD (Mn SOD) acts on superoxide anion to produce hydrogen peroxide (H_2O_2). H_2O_2 is further reduced to water by glutathione (GSH) and catalase [6,16,17]. Similarly, nuclear factor erythroid 2-related factor 2 (Nrf2) is a transcription factor which plays an important role in defense against toxic insults by upregulating various antioxidant enzymes and is also involved in the modulation of mitochondrial function and biogenesis [18]. Reduction in mitochondrial and intracellular ROS and activation of Nrf2 are considered to be beneficial to the mitochondrial function under the oxidative stress. Thus, mitochondria-targeted antioxidants that are highly researched as a therapeutic strategy for the treatment of many neurodegenerative diseases [19].

Methylene blue (MB) is a tricyclic phenothiazine drug that crosses blood brain barrier and reaches to the brain. It has been applied clinically in the treatment of depression, cancer, methemoglobinemia [2,20,21]. It is a redox cycler known to possess antioxidative property along with the ability to reduce tau protein aggregation [20]. MB displayed neuroprotective effects in a variety of neurodegenerative disease models like Alzheimer's disease by inducing autophagy system and attenuating tauopathy; Huntington's disease by modulating Huntingtin aggregation and increasing BDNF RNA, traumatic brain injury by reducing microglial activation [21-23]. We previously showed that MB protected the dopaminergic neurons against MPTP *in vivo* by upregulating neurotrophic factors [2]. However, the role of MB in modulation of apoptosis, oxidative stress and mitochondrial impairment induced by MPP^+ has not been demonstrated yet.

Reducing oxidative stress, and enhancing mitochondrial functions are regarded as potential therapeutic targets for the treatment of PD [24,25]. In this study, we investigated effects of MB on MPP^+-induced oxidative stress, mitochondrial dysfunction and apoptotic cell death. Here we demonstrated that MB protects SH-SY5Y cells from MPP^+-induced toxicity by attenuating oxidative stress, restoring mitochondrial function through the activation of Nrf2 transcription factor via AKT pathway.

2. Materials and methods

2.1. SH-SY5Y cell culture

Human neuroblastoma SH-SY5Y cells were graciously obtained from Professor Jeong Gil Saeng (College of Pharmacy, Keimyung University). The cells were grown in Dulbecco's modified Eagle's medium (cat # SH30243, HyClone Laboratories) supplemented with 10% fetal bovine serum and 1% penicillin/streptomycin at 37 °C, in 5 % CO_2 humidified atmosphere. The cells were grown to a confluence of 80–90% after which the cells were either subcultured after trypsinization with 0.25% trypsin (HyClone Laboratories) or plated into specific cell densities for the treatment of the cells. The cell culture medium was replaced every 2–3 days.

2.2. Neuron-enriched mesencephalic cultures and drug treatment

Neuron-enriched mesencephalic cultures were performed as previously described with some modification [26]. Briefly, C57BL/6N ventral mesencephalon were isolated from the embryonic day 13 (E13) fetal brain and dissected in Leibovitz's L-15 Medium (Welgene, Seoul, Korea). The dissected segments were incubated in 0.01% trypsin solution diluted in Ca^{2+}-, Mg^{2+}-free HBSS (Life Technologies, Rockville, MD, USA) for 10 min at 37 °C and incubated for an additional 5 min at 37 °C in 100 μg/ml DNase I diluted in DMEM medium (Life Technologies). The tissues were mechanically triturated in DMEM medium supplemented with 10% FBS and 100 U/ml penicillin/streptomycin (P/S). The dissociated cells were plated on 8-well slide pre-coated with 100 μg/ml poly-D-lysine and 4 μg/ml laminin at a density of 6×10^5 cells/ml (300 μl/well). The cells were incubated in a humidified incubator at 37 °C, 5% CO_2 for 24 h and replaced with serum-free medium composed of Ham's nutrient mixture (F12-DMEM, Life Technologies) and supplemented with 1% ITS (insulin, transferrin, selenium) and P/S. At DIV 4, the neurons were treated with 10 μM MPP^+ with or without MB and ML385 for 24 h as indicated and processed for immunocytochemical staining. MB was treated 3 h before MPP^+ treatment, and ML385 was treated 1 h before MB treatment.

2.3. Immunocytochemistry and cell counting

Immunocytochemical staining was performed as previously described with some modification [26]. Briefly, 2 days after drug treatment, neurons were fixed with 4% paraformaldehyde for 30 min at 25 °C. The cells were rinsed with PBS and permeabilized by PBS containing 0.2% triton X-100 and 1 % BSA for 5 min at 25 °C and then incubated with anti-tyrosine hydroxylase antibody (TH, Thermo Fisher Scientific) diluted in PBS containing 0.5% BSA for overnight at 4 °C to detect the TH-positive dopaminergic neurons. The cells were rinsed with PBS containing 0.5% BSA and then incubated with biotinylated anti-rabbit IgG (vector laboratories, CA, USA). 1 h later, the cells were rinsed with PBS containing 0.5% BSA, and incubated with pre-incubated avidin–biotin complex (ABC HRP kit, Vector Laboratories) for 1 h at 25 °C. After rinsed twice in 0.1 M phosphate buffer, the cells were incubated in 0.05% 3,3′-diaminobenzidine (Sigma-Aldrich) in 0.1 M phosphate buffer containing 0.003% H_2O_2 to visualize the immunocomplexes. Then, the cells were counterstained with 0.1% cresyl violet (Sigma-Aldrich) and dehydrated. The stained cells were captured under a slide scanner (3DHISTECH, Budapest, Hungary). Images from mesencephalic neuronal culture were analyzed in ImageJ software (National Institutes of Health; https://imagej.nih.gov/ij/). ImageJ with 'Analyze particles' was used to quantify the cell number.

2.4. Cell viability assay

Viability of SH-SY5Y cells was determined by 3-(4,5-dimethylthiazol-2-yl)-5-(3-carboxymethoxyphenyl)-2-(4-sulfophenyl)–2H-tetrazolium (MTS) assay (Cell titer 96 Aqueous One solution cell proliferation Assay, cat # 3580, Promega Corp., Madison, WI, US) as described in previous study [27]. Briefly, at the end of the experiment, 20 ul of the MTS reagent was added to the medium and incubated for 3 h. Then, absorption was read at 490 nm using a microplate reader (Multiskan GO, Thermo Fisher Scientific, Ratastie, Finland) to obtain the viability of the cells expressed as percentage of the control group.

2.5. Caspase-3 activity assay

Caspase-3 activity was assessed using a luminometric assay using caspase-Glo® 3/7 Assay (cat # G8090, Promega Corp., Madison, WI) which is a homogeneous, luminescent assay to measure caspase-3 activities. The assay kit contains a luminogenic caspase-3 substrate in a reagent optimized for caspase activity, luciferase activity and cell lysis. The caspase cleavage of the substrate results in generation of a "glow-type" luminescent signal, produced by luciferase that is proportional to the amount of caspase activity present in the system. After the treatment is completed, 100 μl of Caspase-Glo® 3/7 reagent was added to each well of a white-walled 96-well plate containing cell. Then the plate was incubated at 37 °C for 30 min and caspase activity was detected by measuring luminescence of each sample in a plate-reading luminometer.

2.6. Intracellular and mitochondrial ROS measurement

Intracellular ROS production was measured using the CMH_2DCF-DA probe. After the completion of treatment, the cells were incubated with

5–10 μM CMH_2DCFDA at 37 °C for 30 min and ROS production was detected by measuring fluorescence of oxidized DCF (Fluostar omega, BMG LABTECH; $\lambda_{excitation} = 485$ nm and $\lambda_{emission} = 520$ nm).

Mitochondrial ROS was measured using MitoSOX™ Red mitochondrial superoxide indicator. MitoSOX is a novel cell permeable fluorogenic dye that is rapidly oxidized by superoxide but not by other reactive oxygen species (ROS) and reactive nitrogen species. The oxidized product is highly fluorescent upon binding to nucleic acid. After the completion of treatment, the cells were incubated with 5 μM MitoSOX™ at 37 °C for 30 min and ROS production was detected by measuring fluorescence of oxidized product ($\lambda_{excitation} = 510$ nm and $\lambda_{emission} = 580$ nm).

The fluorescence was measured by microplate reader and a fluorescence microscope using the respective excitation and emission wavelengths and appropriate filters. The fluorescence intensities of the microscopic images [10 images per group, n = 4)] were quantified by Image J software and values were presented as percentages [Threshold values were kept constant for both green and red fluorescence].

2.7. Complex I activity assay

The mitochondrial complex I (NADH oxidase/co-enzyme Q reductase) activity was measured using MitoCheck Complex I Activity Assay kit (cat #700930, Cayman chemical, Ann Arbor, MI, USA) according to the manufacturer's instruction with slight modification. Briefly, in tube A, we added 910 μl of complex I activity assay buffer, 20 μl of 100 nM rotenone, 50 μl of fatty acid free-BSA assay reagent and 20 μl bovine heart mitochondria assay reagent. In tube B, complex I activity assay buffer, NADPH assay reagent and ubiquinone assay reagent were added. 50 μl of the contents of tube A was pipetted into each well of 96-well plate. Then, 20 μl of 5 μM MB and 30 μl of the contents of tube B was added to each well. The plate was placed in plate reader and the absorbance was measured at 340 nm in interval of 30 sec for 30 min at 25 °C. Complex I activity determined by the rate of NADH oxidation which was measured by a decrease in absorbance at 340 nm.

2.8. ATP assay

ATP levels in the cells were determined using CellTiter-Glo luminescent cell viability assay kit (cat # G7572, Promega Corp., Madison, WI, US) which quantitates the ATP as an indicator of the metabolically active cells. The reagent was prepared according to the manufacturer's instruction and luminescence measured in white flat bottom 96-well plates using a luminometer (Fluostar Omega, BMG LABTECH) with an integration time of 1 s. The concentration of ATP was extrapolated from the standard curve using a series of dilution of standard solutions.

2.9. Annexin V FITC apoptosis detection

The BD Pharmingen™ Annexin V FITC apoptosis detection kit (BD Biosciences Pharmingen, USA), was used to detect apoptosis using flow cytometry. The reagent was prepared according to the manufacturer's instruction and percentage of cells within a population actively undergoing apoptosis were determined quantitatively. After the cell treatment, cells were washed twice with 1X cold PBS and then the cells were resuspended in 1X binding buffer at a concentration of $1 \times 10\hat{}6$ cells/ml. 100 μl of the solution (1×10^5 cells) were transferred to a 5 ml culture tube and 5 μl of FITC Annexin V and 5 μl PI were added. Then the cells were gently vortexed and incubated for 15 min at 25 °C in the dark. 400 μl of 1X Binding Buffer were added to each tube and analyzed by flow cytometry within 1 h.

2.10. Measurement of glutathione (GSH) concentration

Change in GSH levels is an important indicator of oxidative stress in the cells leading to cellular death. Thus, GSH measurements were performed using the GSH-Glo™ GSH assay kit (cat # V6911, Promega Corp., Madison, WI, USA) which is a luminescent-based assay for detection and quantification of GSH in cells, based on the conversion of a luciferin derivative into luciferin in the presence of GSH. The experiment was performed according to the manufacturer's instructions. The cells are first lysed in the presence of luciferin-NT substrate and GSH S-transferase enzyme supplied in the kit. GSH in the cells drives the formation of luciferin, which is then converted, into light/signal by the addition of luciferin detection reagent. The signal, thus generated is proportional to the amount of GSH present in the samples. The concentration of cellular GSH was extrapolated from the standard curve using standard solution provided in the kit.

2.11. Measurement of superoxide dismutase (SOD) activity

SOD activity was determined using the SOD colorimetric activity kit (cat # EIASODC, Thermo Fisher Scientific, USA) according to the protocol provided. The cytosolic SOD (Cu/Zn, SOD1) and mitochondrial SOD (Mn, SOD2) were separated through ultracentrifugation. A standard curve was created using the standard provided in the kit and the concentrations of the samples were extrapolated using the standard curve and expressed as unit/mg protein in the sample.

2.12. JC-1 mitochondrial membrane potential (MMP) assay

5,5,6,6′-tetrachloro-1,1′,3,3′ tetraethylbenzimi-dazoylcarbocyanine iodide (JC-1) dye (cat # T3168, ThermoFisher Scientific, USA) was used as a direct measure of the MMP in healthy and apoptotic cells. In healthy cells with normal functioning mitochondria, JC-1 dye, which is a lipophilic cationic dye, can enter into the energetic and negatively charged mitochondria in a concentration dependent manner to form JC-1 aggregates exhibiting a red fluorescence (absorption/emission-585/590 nm). However, in apoptotic cells that have lost their MMP, relatively small amount of JC-1 dye can enter into the mitochondria and retain the green fluorescence of the JC-1 monomers (absorption/emission-510/527 nm).

The red and green fluorescence was measured using a fluorescence plate reader and the ratio of the red:green fluorescence was calculated to give a measure of the MMP in the samples performed in quadruplicates from four independent experiments. The microscopic images were obtained using a fluorescence microscope (Nikon, Melville, NY, USA).

2.13. Western blot analysis

Cell samples were homogenized with ice-cold RIPA lysis buffer, and 1% protease inhibitor cocktail. The tissue homogenate was centrifuged at 4 °C for 20 min at 13,000 rpm, and the supernatant was transferred to a fresh tube. Similarly, nuclear-protein was separated using NE-PER™ nuclear and cytoplasmic extraction reagent (cat # 78833, Thermo Fisher Scientific, USA) according to the manufacturer's protocol. Also, the mitochondria were isolated using Mitochondria Isolation Kit for Cultured Cells (cat # 89874, Thermo Fisher Scientific, USA), as described in the manufacturer's instructions. Protein concentration was determined using BCA protein assay kit (cat # 23225, Thermo Fisher Scientific). Equivalent amount of protein samples were loaded and separated on 12% SDS-polyacrylamide gel by electrophoresis, and transblotted to polyvinylidene difluoride membranes (Millipore Corporation, Temecula, CA). Membranes were blocked with 5% skim milk in Tris-buffered saline (0.1% Tween 20), for 1 h. Then, the membrane was incubated overnight at 4 °C with specific primary antibodies to against Nrf2 (1:2000, Cell Signaling Technology), Cleaved Caspase-3 (1:2000, Cell Signaling Technology), Caspase-3 (1:2000, Cell Signaling Technology), p-JNK (1:2000; Cell Signaling Technology), JNK (1:2000, Cell Signaling Technology), HO-1 (1:2000, ENZO), Bax (1:2000, BD Biosciences), Bcl-2 (1:2000, Cell Signaling Technology), p-53 (1:2000, Cell Signaling Technology), PGC-1α (1:2000,Thermo Fisher Scientific), cyt c

(1:2000, Cell Signaling Technology), β-actin (1:10000, Ab-Frontier) and GAPDH (1:10000, Ab-Frontier). The membrane was incubated with an HRP-labeled secondary antibody for 1 h at 25 °C. Finally, the membrane was incubated with enhanced chemiluminescence reagents (Thermo Fisher Scientific) and exposed in a luminescence image analyzer (Fusion Solo, VilberLourmat, France) to detect the immunoreactive complex. Density of each blot was assessed using GelQuant.Net software.

2.14. siRNA transfection with SH-SY5Y cells

SH-SY5Y cells were transiently transfected with siRNA (Bioneer, Daejeon, Korea) specific for Nrf2 gene or non-specific gene (scramble siRNA) using HiPerfect transfection reagent (cat # 301704, Qiagen, Maryland, USA). The sequences of the siRNA used in this study were depicted in Table 1. Briefly, the cells were plated at $2.5x10^5$ cells in 35-mm culture dishes and incubated overnight. Transfection mixture was prepared and incubated for 20 min at 25 °C. The cells were washed once with plain media and replaced with fresh plain media. The transfection mixture was then added to the each well gently and uniformly. After 6–8 h equal volumes of complete media were added and the cells were further incubated for 24–36 h. The cells were then washed once with 1X PBS and treated as explained in the figure legends. Gene silencing efficiency was measured using western blot analysis after 36 h post transfection. siRNA duplexes were purchased from Bioneer (Daejeon, South Korea).

2.15. Statistical analysis

All values are expressed as the mean ± SEM of multiple independent experiments. Statistical analysis was performed using one-way or two-way ANOVA followed by the Student–Newman–Keuls or Tukey's post-hoc test to calculate statistical differences between various groups (GraphPad Prism 5.0, San Diego, CA, USA). Values of $p<0.05$ were considered statistically significant.

3. Results

3.1. MB protects SH-SY5Y cells against MPP^+-induced apoptotic cell death

MTS assay was carried out to test the protective effect of different concentrations of MB (1, 5, 10 and 20 μM) against MPP^+ toxicity. The cells were pretreated with MB for 3 h followed by MPP^+ for 24 h. MPP^+ caused substantial cell death and treatment with MB significantly reduced MPP^+-induced loss of cells. Among the different doses of MB, 5 μM was found to be the most effective against MPP^+ toxicity, and the dose was chosen for further experiments (Fig. 1A).

Next, western blotting was performed to check the effect of MB against apoptotic markers which are intimately involved in the cell death processes. MPP^+ significantly increased the phosphorylation of JNK and also elevated the levels of p53 and Bax (Fig. 1B-D). These effects of MPP^+ were significantly reversed by MB. In parallel with the results, MPP^+ reduced the anti-apoptotic marker, Bcl-2 and this was drastically counteracted by MB pretreatment (Fig. 1E).

Cyt c is an essential component of the mitochondrial respiratory chain that plays a major role in cell apoptosis. When cyt c is released from mitochondria into cytosol it interacts with apoptotic protease activating factors and initiates the activation cascade of caspases leading to the activation of cell apoptosis [15]. Thus, experiments were performed to assess the translocation of cyt c from mitochondria to cytosol as well as expression pattern of caspase-3. Western blot results revealed that pretreatment of MB significantly lowered the MPP^+-induced translocation of cyt c from mitochondria into the cytosol (Fig. 2A, B). Similarly, assay of caspase-3 activity showed that MB pretreatment attenuated MPP^+-induced activation of caspase-3 (Fig. 2C). Western blot results were consistent with the caspase-3 activity assay (Fig. 2D), suggesting the inhibitory role of MB in MPP^+-induced caspase activation. These results were further supported by annexin V FITC assay using flow cytometry assay where MPP^+ robustly increased the apoptotic rate and it was significantly lowered by MB pretreatment (Fig. 2E, F). All these results indicate that MB reduces MPP^+-mediated apoptotic cell death.

Table 1
The sequences of siRNA used in the study.

Target gene	Primer	Nucleotide sequence (5′-3′)
Nrf2	Sense	GAGACUACCAUGGUUCCAA
	Antisense	UUGGAACCAUGGUAGUCUC
Non-targeting	Sense	CCUACGCCACCAAUUUCGU
	Antisense	ACGAAAUUGGUGGCGUAGG

3.2. MB Reduces MPP^+-induced cytosolic and mitochondrial ROS overgeneration

Intracellular ROS production was assessed by measuring the fluorescence from oxidation of CM-H_2DCFDA to oxidized DCF. Cells were pretreated with MB for 3 h followed by MPP^+ treatment for 24 h. MPP^+ elevated the ROS production considerably, and MB was able to reduce the intracellular ROS in MPP^+ treated cells (Fig. 3A, B). Mitochondrial ROS was measured using MitoSOX red assay kit. MPP^+ raised mitochondrial superoxide generation as shown by increase in red fluorescence level. The overproduction of mitochondrial ROS by MPP^+ was ameliorated by pretreatment of MB (Fig. 3C, D).

3.3. MB Attenuates MPP^+-mediated impairment in mitochondrial function

Mitochondrial membrane potential (MMP) was quantified using the red and green fluorescence produced in JC-1 dye treated cells. MPP^+ significantly reduced MMP as the ratio of red to green fluorescence intensity was decreased. MB pretreatment markedly ameliorated the MPP^+-induced loss of MMP (Fig. 4A). MPP^+ leads to mitochondrial dysfunction primarily by inhibiting complex I activity that results in ATP depletion. Thus, complex I activity was measured with cell-free assay with rotenone, which is another well-known potent mitochondrial complex I inhibitor. The results showed that MB restored rotenone-induced complex I activity inhibition (Fig. 4B). ATP assay results revealed that MB significantly restored ATP levels in MPP^+-treated cells (Fig. 4C).

Next, we checked if MB upregulates PGC-1α level, since it regulates mitochondrial biogenesis, increases the expression of antioxidant enzymes, and is involved in Nrf2 activation [28]. Analyses with western blot showed that MB alone significantly increased PGC-1α expression, while MPP^+ reduced PGC-1α in the cells. Importantly, pretreatment with MB recovered the MPP^+-mediated reduction (Fig. 4D).

3.4. MB induces Nrf2/HO-1 and antioxidants afflicted by MPP^+

Nrf2 transcriptional pathway is known to mediate the induction of antioxidant genes that play an important role in the cellular defence against oxidative stress and its nuclear translocation is required for its activation [29]. Thus, western blot was carried out in the nuclear and cytosolic cell fractions to determine Nrf2 nuclear translocation. Results revealed that Nrf2 nuclear translocation was reduced by MPP^+ treatment which was increased by MB suggesting that MB augments Nrf2 activity that might regulate the antioxidant system in the cells to enhance the cellular survival (Fig. 5A-B). HO-1 is an Nrf2 target gene which was significantly increased by MB treatment in MPP^+-intoxicated cells (Fig. 5C).

Nrf2 is required for maintaining the intracellular redox status by regulating the expression of a number of genes that affect GSH levels [29], and SOD levels [30]. MPP^+ induced a sharp reduction in GSH,

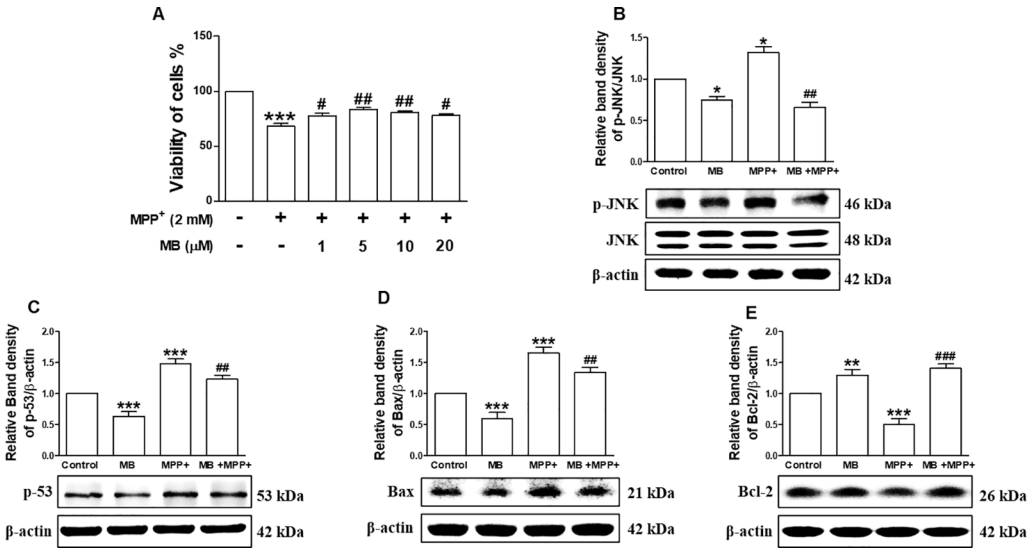

Fig. 1. MB reduces MPP^+-caused cell death and pro-apoptotic molecules. SH-SY5Y neuroblastoma cells were pretreated with four different MB concentrations (1, 5, 10 and 20 μM) followed by 2 mM MPP^+ for the next 24 h. (A) MTS assay was carried out to assess the cell viability. Western blot analysis was performed to determine the protein levels of (B) JNK and p-JNK (C) p-53 (D) Bax (E) Bcl-2 along with β-actin. Quantitative analysis was carried out with GelQuant.Net and GraphPad Prism 5. Values were normalized using either total protein or β-actin, and represent relative to control. $*p < 0.05$ and $**p < 0.01$ and $***p < 0.001$ compared to control, $\#p < 0.05$, $\#\#p < 0.01$ and $\#\#\#p < 0.001$ compared to MPP^+ treated group. All values represent mean ± S.E.M. (n = 4).

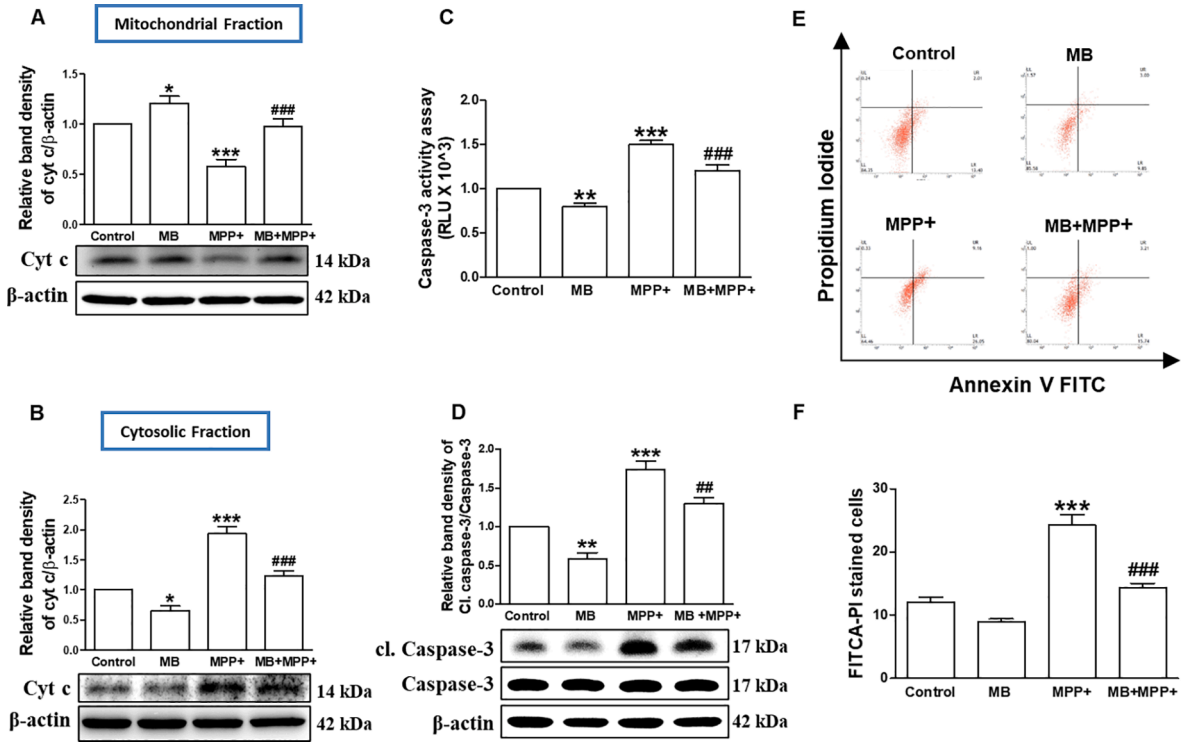

Fig. 2. MB reduces MPP^+-induced cyt c translocation and caspase-3 activation. Cells were pretreated with MB for 3 h followed by 2 mM MPP^+ for next 24 h. Western blot was performed to evaluate the cyt c level in the mitochondria and cytosol (A and B), and the expression of cleaved caspase-3 (D). Apoptotic activation was assessed using caspase-3 activity assay (C) and flow cytometry analysis through Annexin V FITC assay (E and F). Quantitative analysis was carried out with GelQuant. Net and GraphPad Prism 5. Values were normalized using either total protein or β-actin, and represent relative to control. For caspase-3 activity assay, luminescence of the samples was measured and values were calculated relative to the control group. $*p < 0.05$, $**p < 0.01$ and $***p < 0.001$ compared to control, $\#\#p < 0.01$, $\#\#\#p < 0.001$, compared to MPP^+ treated group. Values are expressed relative to untreated control and represented as mean ± SEM of four independent experiments performed in triplicates (n = 4).

cytosolic SOD and mitochondrial SOD levels in SH-SY5Y cells and MB significantly increased the level of these antioxidants in the MPP^+-treated cells suggesting that Nrf2 activation followed by enhancement of these antioxidants in the cells might be responsible in reducing the toxic effects of MPP^+ (Fig. 5D-F).

3.5. MB exerts neuroprotection through Nrf2 pathway

We performed experiments to assess whether the neuroprotection shown by MB was dependent on Nrf2 activation. For this we used Nrf2 inhibitor, ML385 and siRNA targeting Nrf2 gene to inhibit the Nrf2 activity in the SH-SY5Y neuroblasoma cells. Cell viability test performed with Nrf2 inhibitor revealed that the protective effects of MB against MPP^+ toxicity was abolished in presence of ML385 (Fig. 6A) or Nrf2-

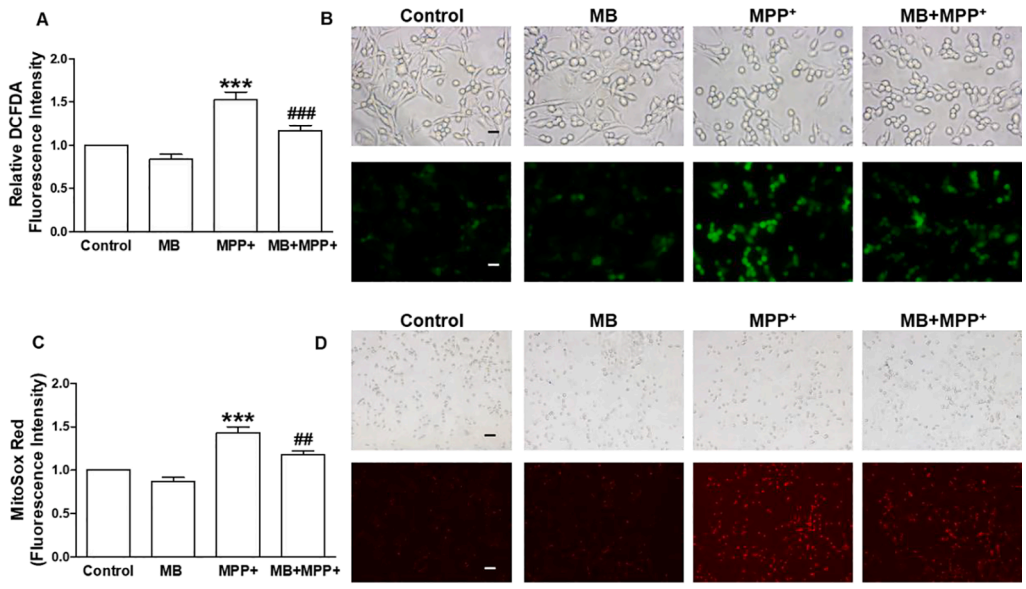

Fig. 3. MB reduces intracellular and mitochondrial ROS in SH-SY5Y cells caused by MPP^+. The SH-SY5Y cells were pretreated with MB as indicated for 2 h followed by 2 mM MPP^+ for 30 min. (A-B) The cells were further treated with 10 μM CM-H_2DCFDA general oxidative stress indicator reagent or for 30 min and the fluorescence intensity was measured and visualized under a fluorescence microscope (magnification: 20x, scale bar: 25 μm). (C-D) The cells were further treated 5 μM MitoSOX™ Red mitochondrial superoxide indicator reagent for 30 min and the fluorescence intensity was measured and visualized under a fluorescence microscope (magnification: 10X, scale bar: 50 μm). ***$p < 0.001$ as compared to control group, ##$p < 0.01$ and ###$p < 0.001$ as compared to the MPP^+ treated group. All values represent mean ± S.E.M from four independent experiments performed in quadruplicates (n = 4).

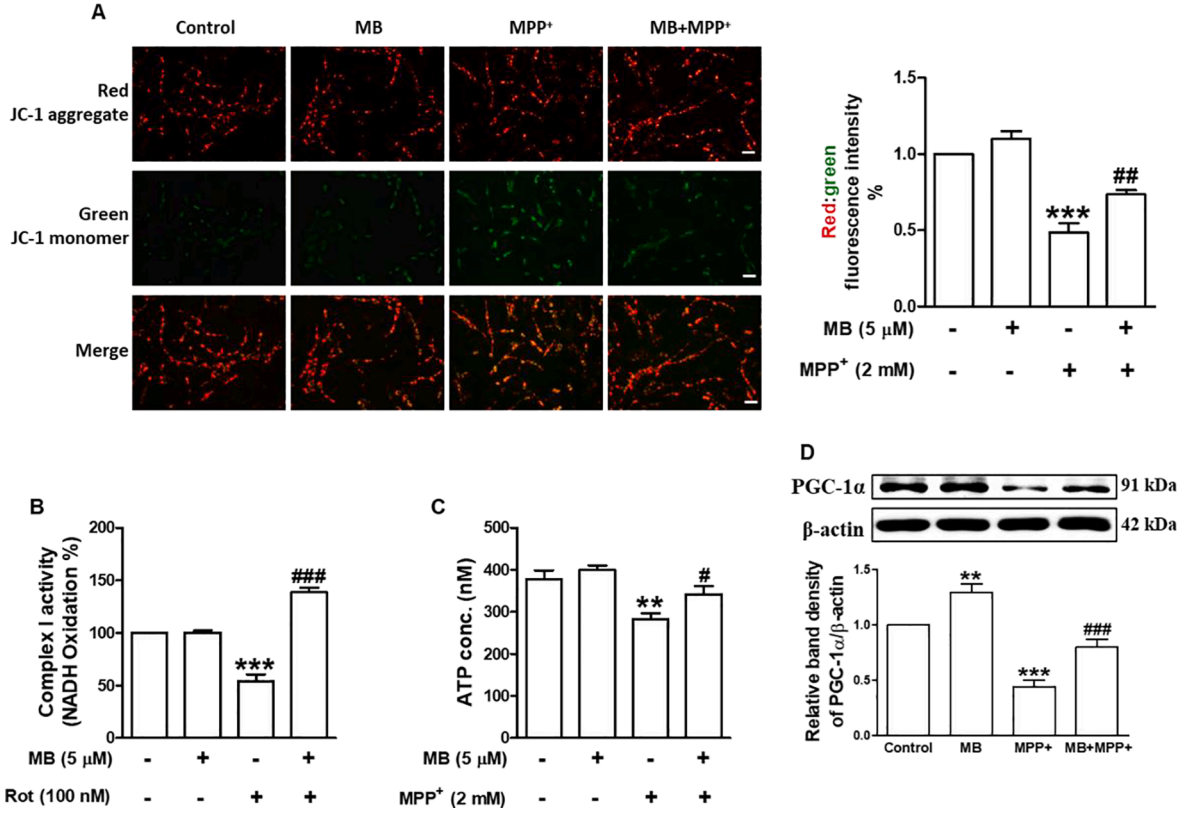

Fig. 4. MB attenuates mitochondrial dysfunction caused by MPP^+. The cells were pretreated with MB for 3 h followed by 2 mM MPP^+ treatment for 24 h. The cells were stained with fluorescent JC-1 dye and the red and green fluorescence was measured either by (A) fluorescence microscope or by microplate reader. The ratio of red and green fluorescence as obtained as values relative to control group. (B) Complex I activity assay was measured using Mitocheck Complex I activity assay kit and values were represented as percentage of controls in the cell free assay. (C) ATP levels were measured in the cells after completion of the treatments. The ATP concentration was extrapolated from the standard curve. (D) Western blot analysis was performed to determine the protein levels of PGC-1α. Magnification 200X: scale bar − 25 μm. **$p < 0.01$ and ***$p < 0.001$, compared to control group, #$p < 0.05$, ##$p < 0.01$ and ###$p < 0.001$ compared to the MPP^+ treated group, ###$p < 0.001$ compared to rotenone group. All values represent mean ± S.E.M from four independent experiments performed in quadruplicates (n = 4).

siRNA (Fig. 6B) suggesting that MB requires Nrf2 activation for the neuroprotection. To further confirm the role of Nrf2 in the neuroprotection, we employed the mescencephalic neuronal cell culture. Immunocytochemical stainings for TH showed that MPP^+ evidently decreased the number of TH + neurons and pretreament of MB significantly rescued the neurons from MPP^+-caused injury. Importantly, addition of ML385 completely diminished the protective effects of MB indicating that the neuroprotective effects of MB is predominantly

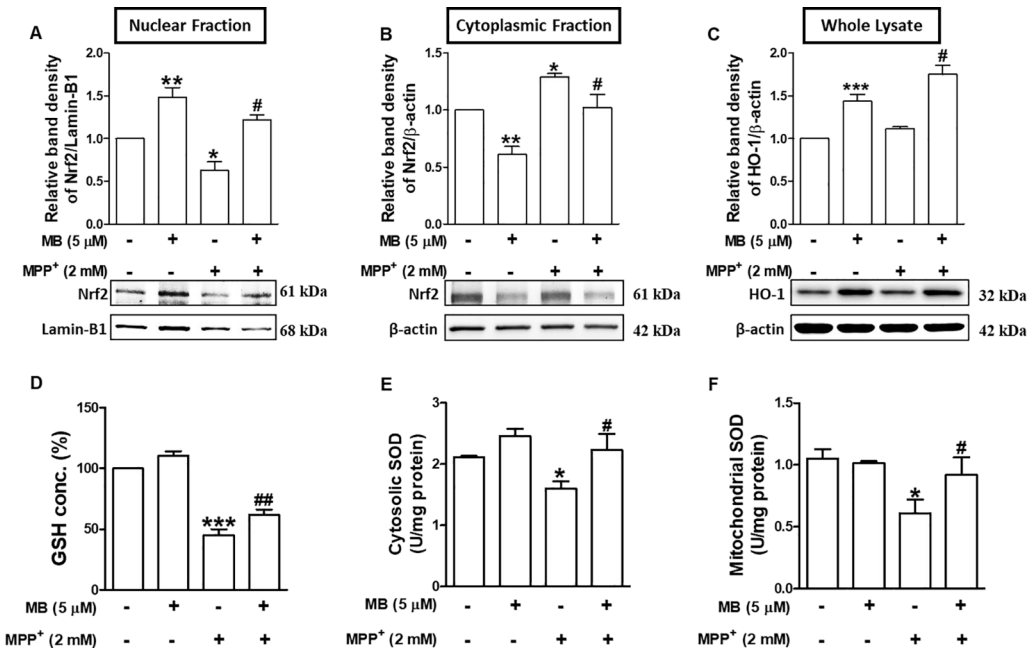

Fig. 5. MB increases antioxidant system and upregulates Nrf2/HO-1 pathway in SH-SY5Y cells. The cells were pretreated with MB for 3 h followed by 2 mM MPP^+ treatment for 24 h. Antioxidants including GSH, cytosolic SOD and mitochondrial SOD were evaluated. (A) GSH levels were quantified relative to control. (B) The cytosolic and (C) mitochondrial SOD activity in the cells were measured and normalized to total protein in the samples. Western blot was performed to check levels of (D) nuclear Nrf2, (E) cytosolic Nrf2, and (F) HO-1. Quantitative analysis was carried out with GelQuant.Net and GraphPad Prism 5. Values were normalized using either total protein or β-actin, and represent relative to control. $*p < 0.05$, $**p < 0.01$, $***p < 0.001$ compared to control group, $\#p < 0.05$ and $\#\#p < 0.01$ compared to the MPP^+ treated group. All values represent mean ± S.E.M. from four independent experiments performed in quadruplicates (n = 4).

mediated by Nrf2 (Fig. 6C). Next, western blot was performed to determine the role of HO-1 activation by MB against MPP^+ toxicity during Nrf2 inhibition. Surprisingly, the western blot results showed that the MB-induced rise in HO-1 expression in MPP^+ intoxicated cell was altered neither in the presence of ML385 nor in the silenced condition, suggesting that the induction of HO-1 by MB was not associated with Nrf2 activation and indicating that HO-1 is not directly involved in MB's protective effect (Fig. 6D, E).

3.6. Involvement of AKT signaling pathway in MB-induced Nrf2 activation

Nrf2 inhibition reversed the neuroprotective property of MB implying that MB depends on Nrf2 to show protection against MPP^+. Thus, possible mechanism behind the activation of Nrf2 by MB was investigated. Experiments were performed with ERK inhibitor (U0126) and AKT inhibitor (10-DEBC) to determine their involvement. Many research studies showed that ERK and AKT activate Nrf2 pathway to provide cytoprotection [31,32]. The cell viability experiments demonstrated that the neuroprotection shown by MB against MPP^+ was abolished by AKT inhibitor but not by ERK inhibitor (Fig. 7A). The results were further supported by western blot experiments. The MPP^+-induced reduction in Nrf2 expression level that was reversed by MB pretreatment was obliterated by AKT inhibition but not by ERK inhibition suggesting that the activation of Nrf2 by MB was dependent on AKT pathway rather than ERK pathway (Fig. 7B, C).

4. Discussion

In this research, neuroprotective effect of MB against MPP^+ neurotoxicity was evaluated. MB clearly exhibited neuroprotection against MPP^+ in SH-SY5Y cells and mescencephalic TH + neurons, possibly by reducing production of ROS and enhancing mitochondrial function. MB significantly induced Nrf2 in the cells along with the upregulation of antioxidant enzymes and provided mitochondrial protection against MPP^+. We also demonstrated that MB activated AKT signaling to induce Nrf2 pathway and provide neuroprotection in SH-SY5Y cells.

MPTP is a neurotoxin that can mimic parkinsonism like symptoms. It readily accumulates in mitochondria and inhibits mitochondrial complex I, disrupts ATP production, increases ROS generation finally leading to neuronal death. Thus, the mechanism behind MPP^+-induced death involves multiple deleterious signals including pro-apoptotic pathways which include cyt c translocation from mitochondria, activation of caspases, p53, Bax, JNK and Bcl-2 family members [4,17]. In this study, MB pretreatment protected the cells against MPP^+-induced apoptotic cell death via inhibition of cyt c release from mitochondria into cytosol and caspase-3, p53, Bax and JNK activation, and increasing the Bcl-2 levels (Figs. 1 and 2).

About 1–2% of the oxygen is converted to superoxide anion mainly in the mitochondrial complex I and III. MnSOD converts superoxide anion to hydrogen peroxide which is further detoxified by catalase. The imbalance between ROS production and antioxidant activity causes progressive oxidative stress [17]. MPP^+ inhibits mitochondrial complex I causing overproduction of ROS, and diminishing antioxidant system including GSH and SOD. The cytosolic SOD (Cu-Zn-SOD or SOD1) or mitochondrial SOD (Mn-SOD or SOD2) acts on superoxide anion to produce H_2O_2 which is further reduced to water by GSH and catalase [6,16,17]. Studies have shown that antioxidant Cu/Zn-SOD enzyme and GSH peroxidase have protective effects against MPTP toxicity [5]. Therefore, GSH and SOD are essential to protect the neurons in the brain from the oxidative stress-induced damage. MB is a redox agent which has ability to penetrate cellular and mitochondrial membranes and accumulate within mitochondria. It prevents the formation of superoxide and nitric oxide in mitochondria and is also able to improve brain oxidative metabolism by enhancing mitochondrial oxygen consumption [33]. MB has proven its anti-oxidative effects in various cell and animal models involving oxidative stress by increasing GSH, SOD activity, mRNA expression of various redoxins and phase-2 antioxidant enzymes such as thioredoxins, NADPH quinone oxidoreductase, and enhancing heme synthesis and mitochondrial respiration [20]. In our study, MB significantly reduced the intracellular and mitochondrial ROS and enhanced MPP^+-induced reduction of cellular GSH and SOD suggesting a potent antioxidative defense mechanism of MB against MPP^+.

Mitochondrial dysfunction and oxidative stress are known to contribute to the degeneration of neurons in PD [34]. MPP^+ disseminates its toxic effects primarily by disrupting mitochondrial electron transport chain (ETC) and production of ROS. Therefore, it is important to restore ETC function and block ROS production. According to the Liu et. al, Coenzyme Q10 functions as an endogenous co-enzyme of ETC proteins and ROS scavenger that have a vital role in maintaining the

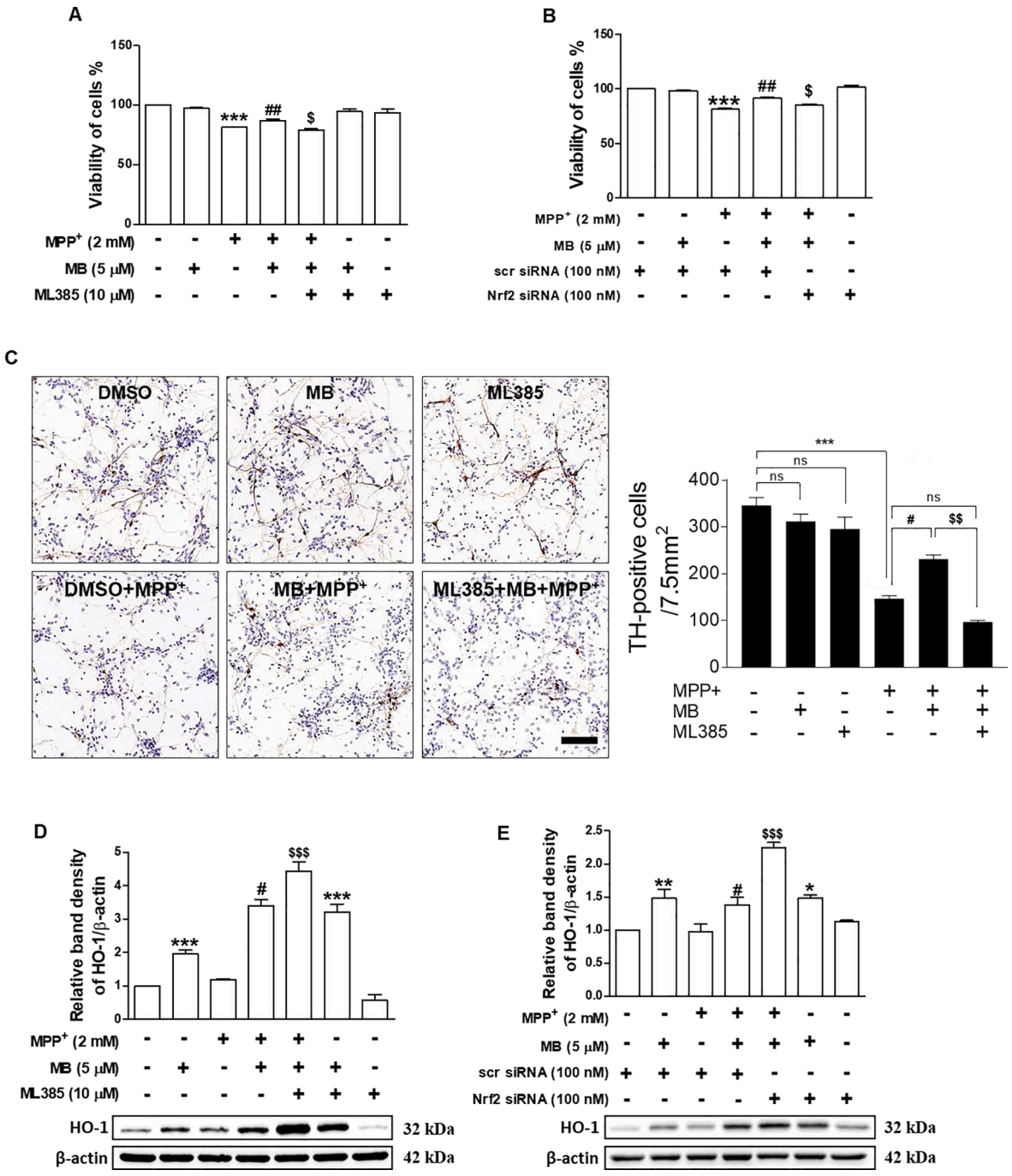

Fig. 6. The neuroprotective effect of MB is dependent on Nrf2 activity. SH-SY5Y neuroblastoma cells and/or the mesencephalic primary cells were treated with ML385 or siRNA againt Nrf2 gene, and then MB. Finally, the cells were exposed to MPP^+ for 24 h. MTS assay or immunocytochemical staining for TH were performed to measure the viability of SH-SY5Y neuroblastoma cells exposed to (A) ML385, the Nrf2 inhibitor or (B) siRNA against Nrf2 gene, and of (C) the mesencephalic primary cells exposed to ML385. Western blot was carried out to analyze levels of HO-1 expression in SH-SY5Y cells exposed to (D) ML385 or (E) siRNA against Nrf2 gene. Quantitative analysis was carried out with GelQuant.Net and GraphPad Prism 5. Values were normalized using β-actin, and represent relative to control. $*p < 0.05$, $**p < 0.01$, $***p < 0.001$ compared to control group, $\#p < 0.05$ and $\#\#p < 0.01$ compared to the MPP^+ treated group, $\$p < 0.05$, $\$\$\$p < 0.001$ compared to the MPP^+ and MB treated group. All values represent mean ± S.E.M. from four independent experiments performed in quadruplicates (n = 4).

integrity of mitochondrial respiration and clearance of free radicals. It produces its protective effects by inhibiting mitochondrial dysfunction, and ROS production induced by neurotoxins like paraquat, rotenone and MPTP both *in vitro* and *in vivo* model [35]. Creatine attenuated MPP^+-mediated toxicity in embryonic ventral mesencephalic neurons by buffering cellular ATP and preventing mitochondrial permeability transition pore opening [8]. Another compound rasagiline possesses multiple effects on mitochondrial function, including stabilization of mitochondrial membrane potential and might have a disease-modifying effect based on clinical trial evidences [8].

In our study, MB was able to restore the complex I activity suggesting that MB might be an ideal pharmacological intervention that will not only reduce oxidative stress in the vulnerable cells, but also restore mitochondrial function to provide greater protection in susceptible cells. In line with the restoration of complex I activity, MB reestablished MPP^+-mediated ATP reduction in cells. MB also reversed MPP^+-induced

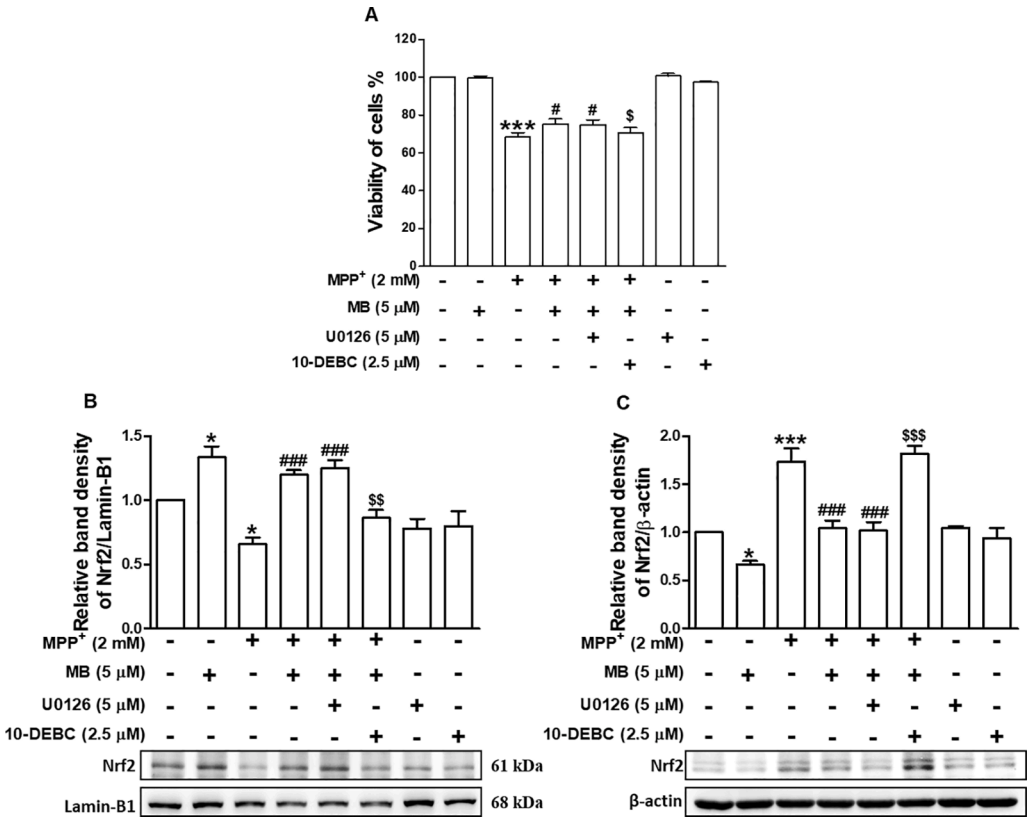

Fig. 7. Involvement of AKT signaling in MB-induced Nrf2 activation. SH-SY5Y cells were treated with different inhibitors i.e. 10-DEBC (2.5 μM) and U0126 (5 μM) for 1 h followed by pretreatment of MB for 3 h and MPP^+ was added and incubated for 24 h. (A) MTS assay was performed to check the cell viability with AKT and ERK inhibitor. Western blot analyses were performed in (B) nuclear lysate and (C) cytosolic fraction to determine the Nrf2 activation. $*p < 0.05$, and $***p < 0.001$, compared to control group, $\#p < 0.05$, and $\#\#\#p < 0.001$ compared to the MPP^+-treated group, $\$p < 0.05$, $\$\$p < 0.01$, and $\$\$\$p < 0.001$ compared to the MB and MPP^+-treated group. All values represent mean ± S.E.M from four independent experiments (n = 4).

mitochondrial membrane potential loss in the cells as observed in JC-1 assay that gives a measure of mitochondrial health. Mitochondrial biogenesis is activated during mitochondrial damage, which indispensably supports energy-dependent cell processes, including those involved in the repair of cell and tissue damage [14]. PGC-1α is a transcriptional coactivator which induces mitochondrial biogenesis [28]. Here, MB increased PGC-1α level in MPP^+ treated cells suggesting PGC-1α induction by MB might be associated with mitochondrial protection and the neuroprotective effects.

We showed that MB caused a clear activation of Nrf2 pathway which is the major mechanism of maintaining the oxidative balance in the cells. MB-induced nuclear translocation of Nrf2 was accompanied by increase in HO-1, GSH, mitochondrial and cytosolic SOD levels. HO-1 is one of the various target enzymes that is activated via Nrf2 induction and it has been shown to be protective by providing mitochondrial protection [36]. Consistent with our current study, MB has been shown to upregulate Nrf2/ARE pathway and attenuate tau-mediated neurotoxicity [20]. In the presence of Nrf2 inhibitor or siRNA targeting Nrf2 gene, MB's protective effect was diminished with upregulation of HO-1 suggesting that protective effect of MB might not be associated with HO-1 upregulation. Rather than HO-1 upregulation, induction of antioxidants and PGC-1α might be responsible for the neuroprotective property of MB. However, we cannot rule out the possibility that MB might exert the neuroprotective effects through HO-1, since the enzyme could contribute to the cell defence via attenuating oxidative stress and neuroinflammatory responses [37]. The observation also indicates that MB increases HO-1 expression via Nrf2-independent pathway. Indeed, HO-1expression can be regulated by other than Nrf2 such as activator protein-1, hypoxia-inducible factor, and Jun N-terminal kinase [38].

Phosphorylation of Nrf2 at serine and threonine by protein kinases such as AKT and ERK releases Nrf2 from Keap1 to enhance its nuclear translocation and transactivation of phase II detoxifying enzymes [39]. Thus, we investigated which of these kinases was required for the Nrf2 activation by MB. The results demonstrated that MB required AKT activation in order to activate Nrf2 and show protection against MPP^+ toxic effects. However, ERK-activation was not compulsory for the NRf2 activation and neuroprotection imparted by MB.

In conclusion, MB demonstrated neuroprotective effects against MPP^+-induced harmful effects by reducing oxidative stress and improving mitochondrial function via Nrf2 activation. This study also demonstrates that the effects were mediated by activating Nrf2 through the AKT signaling pathway. Thus, this study further substantiates MB as a potential therapeutic agent in the treatment of neurodegenerative diseases such as PD which are linked to mitochondrial dysfunction and oxidative stress.

Declaration of Competing Interest

The authors declare that they have no known competing financial interests or personal relationships that could have appeared to influence the work reported in this paper.

Acknowledgements

The present study was supported by the Basic Science Research Program through the National Research Foundation of Korea funded by the Ministry of Education (2018R1D1A3B07049570 to D.Y. Choi), KBRI basic research program through Korea Brain Research Institute funded by Ministry of Science and ICT (21-BR-02-16) and National Research Foundation of Korea (NRF) grant funded by the Korea Government (2020R1F1A1075547, 2021R1F1A1049849 to J. Kim).

References

[1] R. Cacabelos, Parkinson's disease: from pathogenesis to pharmacogenomics, Int. J. Mol. Sci. 18 (3) (2017) 551.

[2] S. Bhurtel, N. Katila, S. Neupane, S. Srivastav, P.-H. Park, D.-Y. Choi, Methylene blue protects dopaminergic neurons against MPTP induced neurotoxicity by

upregulating brain derived neurotrophic factor, Ann. N. Y. Acad. Sci. 1431 (1) (2018) 58–71.
[3] J. Lotharius, P. Brundin, Pathogenesis of Parkinson's disease: dopamine, vesicles and α-synuclein, Nat. Rev. Neurosci. 3 (12) (2002) 932–942.
[4] S.R. Subramaniam, M.-F. Chesselet, Mitochondrial dysfunction and oxidative stress in Parkinson's disease, Prog. Neurobiol. 106-107 (2013) 17–32.
[5] T.N. Martinez, J.T. Greenamyre, Toxin models of mitochondrial dysfunction in Parkinson's disease, Antioxid. Redox Signal. 16 (9) (2012) 920–934.
[6] M.H. Yan, X. Wang, X. Zhu, Mitochondrial defects and oxidative stress in Alzheimer disease and Parkinson disease, Free Radical Biol. Med. 62 (2013) 90–101.
[7] G.E. Meredith, D.J. Rademacher, MPTP mouse models of Parkinson's disease: an update, J. Parkinson's Disease 1 (1) (2011) 19–33.
[8] C. Henchcliffe, M.F. Beal, Mitochondrial biology and oxidative stress in Parkinson disease pathogenesis, Nat. Rev. Neurol. 4 (11) (2008) 600–609.
[9] M.T. Lin, M.F. Beal, Mitochondrial dysfunction and oxidative stress in neurodegenerative diseases, Nature 443 (7113) (2006) 787–795.
[10] V.M.P. Devoto, T.L. Falzone, Mitochondrial dynamics in Parkinson's disease: a role for α-synuclein? Dis. Models Mech. 10 (9) (2017) 1075–1087.
[11] D.N. Hauser, T.G. Hastings, Mitochondrial dysfunction and oxidative stress in Parkinson's disease and monogenic parkinsonism, Neurobiol. Dis. 51 (2013) 35–42.
[12] B. Zheng, Z. Liao, J.J. Locascio, K.A. Lesniak, S.S. Roderick, M.L. Watt, A.C. Eklund, Y. Zhang-James, P.D. Kim, M.A. Hauser, E. Grünblatt, L.B. Moran, S.A. Mandel, P. Riederer, R.M. Miller, H.J. Federoff, U. Wüllner, S. Papapetropoulos, M. B. Youdim, I. Cantuti-Castelvetri, A.B. Young, J.M. Vance, R.L. Davis, J.C. Hedreen, C.H. Adler, T.G. Beach, M.B. Graeber, F.A. Middleton, J.-C. Rochet, C.R. Scherzer, Global PD Gene Expression (GPEX) Consortium, PGC-1α, a potential therapeutic target for early intervention in Parkinson's disease, Sci. Transl. Med. 2 (52) (2010) 52ra73.
[13] M. Weng, X. Xie, C. Liu, K.-L. Lim, C.-wu. Zhang, L. Li, The sources of reactive oxygen species and its possible role in the pathogenesis of Parkinson's disease, Parkinson's Dis. 2018 (2018) 1–9.
[14] S.-D. Chen, D.-I. Yang, T.-K. Lin, F.-Z. Shaw, C.-W. Liou, Y.-C. Chuang, Roles of oxidative stress, apoptosis, PGC-1α and mitochondrial biogenesis in cerebral ischemia, Int. J. Mol. Sci. 12 (10) (2011) 7199–7215.
[15] J. Wan, H.A. Kalpage, A. Vaishnav, J. Liu, I. Lee, G. Mahapatra, A.A. Turner, M.P. Zurek, Q. Ji, C.T. Moraes, Regulation of respiration and apoptosis by cytochrome c Threonine 58 phosphorylation, Scientific reports 9(1) (2019) 1-16.
[16] L. Wang, Q. Duan, T. Wang, M. Ahmed, N. Zhang, Y. Li, L. Li, X. Yao, Mitochondrial respiratory chain inhibitors involved in ROS production induced by acute high concentrations of iodide and the effects of SOD as a protective factor, Oxid. Med. Cell. Longevity 2015 (2015) 1–14.
[17] K. Facecchia, L.-A. Fochesato, S.D. Ray, S.J. Stohs, S. Pandey, Oxidative toxicity in neurodegenerative diseases: role of mitochondrial dysfunction and therapeutic strategies, Journal of toxicology 2011 (2011) 1–12.
[18] M.S. Brandes, N.E. Gray, NRF2 as a Therapeutic Target in Neurodegenerative Diseases, ASN Neuro 12 (2020) 1759091419899782.
[19] N. Kelsey, W. Hulick, A. Winter, E. Ross, D. Linseman, Neuroprotective effects of anthocyanins on apoptosis induced by mitochondrial oxidative stress, Nutrit. Neurosci. 14 (6) (2011) 249–259.
[20] C. Stack, S. Jainuddin, C. Elipenahli, M. Gerges, N. Starkova, A.A. Starkov, M. Jové, M. Portero-Otin, N. Launay, A. Pujol, Methylene blue upregulates Nrf2/ARE genes and prevents tau-related neurotoxicity, Human molecular genetics 23(14) (2014) 3716-3732.
[21] E.E. Congdon, J.W. Wu, N. Myeku, Y.H. Figueroa, M. Herman, P.S. Marinec, J. E. Gestwicki, C.A. Dickey, W.H. Yu, K.E. Duff, Methylthioninium chloride (methylene blue) induces autophagy and attenuates tauopathy in vitro and in vivo, Autophagy 8 (4) (2012) 609–622.
[22] E.M. Sontag, G.P. Lotz, N. Agrawal, A. Tran, R. Aron, G. Yang, M. Necula, A. Lau, S. Finkbeiner, C. Glabe, Methylene blue modulates huntingtin aggregation intermediates and is protective in Huntington's disease models, J. Neurosci. 32 (32) (2012) 11109–11119.
[23] M. Zhao, F. Liang, H. Xu, W. Yan, J. Zhang, Methylene blue exerts a neuroprotective effect against traumatic brain injury by promoting autophagy and inhibiting microglial activation, Mol. Med. Rep. 13 (1) (2016) 13–20.
[24] B. Thomas, M.F. Beal, Mitochondrial therapies for Parkinson's disease, Mov Disord 25 Suppl 1 (Suppl 1) (2010) S155–S160.
[25] R. Filograna, M. Beltramini, L. Bubacco, M. Bisaglia, Anti-oxidants in parkinson's disease therapy: A critical point of view, Curr. Neuropharmacol. 14 (3) (2016) 260–271.
[26] S.R. Kim, E.S. Chung, E. Bok, H.H. Baik, Y.C. Chung, S.Y. Won, E. Joe, T.H. Kim, S. S. Kim, M.Y. Jin, S.H. Choi, B.K. Jin, Prothrombin kringle-2 induces death of mesencephalic dopaminergic neurons in vivo and in vitro via microglial activation, J. Neurosci. Res. 88 (7) (2010) 1537–1548.
[27] N. Katila, S. Bhurtel, S. Shadfar, S. Srivastav, S. Neupane, U. Ojha, G.-S. Jeong, D.-Y. Choi, Metformin lowers α-synuclein phosphorylation and upregulates neurotrophic factor in the MPTP mouse model of Parkinson's disease, Neuropharmacology 125 (Supplement C) (2017) 396–407.
[28] S. Austin, J. St-Pierre, PGC1α and mitochondrial metabolism–emerging concepts and relevance in ageing and neurodegenerative disorders, J. Cell Sci. 125 (21) (2012) 4963–4971.
[29] K. Yama, K. Sato, N. Abe, Y. Murao, R. Tatsunami, Y. Tampo, Epalrestat increases glutathione, thioredoxin, and heme oxygenase-1 by stimulating Nrf2 pathway in endothelial cells, Redox Biol. 4 (2015) 87–96.
[30] A.R. Vasconcelos, N.B. dos Santos, C. Scavone, C.D. Munhoz, Nrf2/ARE Pathway Modulation by Dietary Energy Regulation in Neurological Disorders, Front. Pharmacol. 10 (33) (2019).
[31] K.C. Kim, K.A. Kang, R. Zhang, M.J. Piao, G.Y. Kim, M.Y. Kang, S.J. Lee, N.H. Lee, Y.-J. Surh, J.W. Hyun, Up-regulation of Nrf2-mediated heme oxygenase-1 expression by eckol, a phlorotannin compound, through activation of Erk and PI3K/Akt, Int. J. Biochem. Cell Biol. 42 (2) (2010) 297–305.
[32] X. Yu, N. Song, X. Guo, H. Jiang, H. Zhang, J. Xie, Differences in vulnerability of neurons and astrocytes to heme oxygenase-1 modulation: implications for mitochondrial ferritin, Sci. Rep. 6 (2016) 24200.
[33] X. Zhang, J. C. Rojas, F. Gonzalez-Lima, Methylene blue prevents neurodegeneration caused by rotenone in the retina, Neurotox. Res. 9 (1) (2006) 47–57.
[34] V. Dias, E. Junn, M.M. Mouradian, The role of oxidative stress in Parkinson's disease, J. Parkinson's Dis. 3 (4) (2013) 461–491.
[35] X.L. Liu, Y.D. Wang, X.M. Yu, D.W. Li, G.R. Li, Mitochondria-mediated damage to dopaminergic neurons in Parkinson's disease, Int. J. Mol. Med. 41 (2) (2018) 615–623.
[36] A.L. Chenet, A.R. Duarte, F.J.S. de Almeida, Cláudia.M.B. Andrade, M.R. de Oliveira, Carvacrol depends on heme oxygenase-1 (HO-1) to exert antioxidant, anti-inflammatory, and mitochondria-related protection in the human neuroblastoma SH-SY5Y cells line exposed to hydrogen peroxide, Neurochem. Res. 44 (4) (2019) 884–896.
[37] A. Jazwa, A. Cuadrado, Targeting heme oxygenase-1 for neuroprotection and neuroinflammation in neurodegenerative diseases, Curr. Drug Targets 11 (12) (2010) 1517–1531.
[38] A.M. Choi, J. Alam, Heme oxygenase-1: function, regulation, and implication of a novel stress-inducible protein in oxidant-induced lung injury, Am. J. Respir. Cell Mol. Biol. 15 (1) (1996) 9–19.
[39] M.J. Bak, V.-L. Truong, S.-Y. Ko, X.N.G. Nguyen, M. Jun, S.-G. Hong, J.-W. Lee, W.-S. Jeong, Induction of Nrf2/ARE-mediated cytoprotective genes by red ginseng oil through ASK1-MKK4/7-JNK and p38 MAPK signaling pathways in HepG2 cells, J. Ginseng Res. 40 (4) (2016) 423–430.